1992

Performance Analysis of Hermetic Scroll Compressors

K. Suefuji
Hitachi

M. Shiibayashi
Hitachi

K. Tojo
Hitachi

PERFORMANCE ANALYSIS OF HERMETIC SCROLL COMPRESSORS

Kazutaka Suefuji and Masao Shiibayashi
Mechanical Engineering Research Laboratory, Hitachi, Ltd.
390, Muramatsu, Shimizu-Shi, Shizuoka-Ken, Japan

Kenji Tojo
Shimizu Works, Hitachi, Ltd.
390, Muramatsu, Shimizu-Shi, Shizuoka-Ken, Japan

ABSTRACT

This paper presents a practical method of calculating hermetic scroll compressor performance, considering mechanical loss, leakage loss and heat exchange in the compressor shell. Mechanical friction losses due to fluid resistance of moving parts in the compressor, such as the balancing weight and the orbiting scroll, are considered and estimated. Heat exchange of the refrigerant gas between compressor components is calculated using a simplified thermal analysis model.

The results of these calculations are compared with some measured data. The calculated adiabatic efficiencies agree with the measured values within 3% error, and the calculated discharge gas temperatures agree with the measured values within 3K error, in the revolutionary range from 20 Hz to 150 Hz.

INTRODUCTION

Recently, capacity controllable air conditioners have become popular in association with the demands for improved energy savings and amenities. Therefore, due to the expanding operating frequency range of compressor which are used in air conditioners, it has become necessary to precisely predict compressor performance. However, simulating the compressor behavior is difficult under wide operating conditions. To this day, only some approximated analyses have been attempted on subjects affecting compressor performance. Mechanical forces and losses were clarified peculiar to individual compressor mechanisms [1], [2]. It was additionally pointed out that the deformation of scroll effectively minimizes leakage loss and friction loss [3].

Since scroll compressors for air conditioners first came onto the market in 1983, the self-adjusting support mechanism has been adopted to maintain the contact of the orbiting scroll and the fixed scroll [4]. A high pressure side hermetic shell has been adopted and combined with the above mechanism. This construction improves efficiency and simplifies parts design. However, fluid resistance losses have increased in the back pressure chamber with this construction. Furthermore, the heat exchange between high temperature gas, oil and low temperature suction gas has resulted in thermal loss on the flow rate and the work [5].

To analyze compressor performance over a wide range of operating conditions, and to improve compressor efficiency, several unknown factors are calculated by a new method. This paper presents a method of accurately simulating performance, focusing on leakage loss, fluid resistance losses and

thermal characteristics. The result of an analysis on how to improve the performance is also shown.

NOMENCLATURES

a	sound speed of air
A	sectional area of passage , heat transfer area
c_p	specific heat at constant pressure
D	diameter of pipe
D_{OS}	diameter of orbiting scroll end plate
G	mass flow rate
H_B	height of balancing weight
H_{OS}	height of orbiting scroll end plate
L	length of heat conduction line
m_g	mass of gas
M	Mach 's number
n	polytropic index
P, p	pressure
P_o	pressure when flow velocity is 0
r_1	inner radius of balancing weight
r_2	outer radius of balancing weight
S	sectional area of heat conduction line
t	time
T	temperature
V_c	volume of compression chamber
x	distance
α	heat transfer coefficient
ε	orbiting radius
κ	specific heat ratio
λ	coefficient of wall friction , heat conductivity
ρ	density
ρ_o	density when flow velocity is 0
ω	angle speed
ξ	flow out coefficient
ζ	friction loss coefficient

GENERAL MODELING OF THE COMPRESSORS FOR PERFORMANCE ANALYSIS

Figure 1 is a sectional view of a scroll compressor. This compressor consists of a fixed scroll, an orbiting scroll, an Oldham's coupling ring, a crank shaft and a frame; the orbiting scroll is supported by a self-adjusting support mechanism. The pressure in the back chamber of the orbiting scroll is maintained

at an intermediate range between suction pressure and discharge pressure. The back pressure pushes the orbiting scroll toward the fixed scroll to maintain the sealing of the compression chambers. The discharge port of the fixed scroll is opened in the hermetic shell. The oil is supplied to bearings and frictional surfaces by a differential pressure between the discharge gas and the intermediate pressure gas in the back pressure chamber.

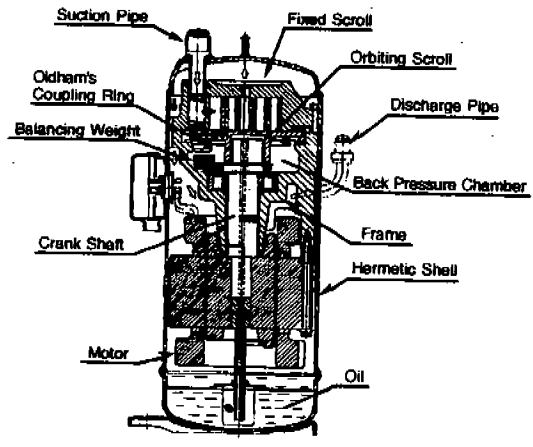

Fig. 1 Scroll compressor

This analysis considers the following power losses.

(1) Compression loss: Due to difference in built-in volume ratio.

(2) Bearing losses: This compressor has three bearings, and loss for each is calculated by experimental equations.

(3) Mechanical friction loss of a thrust bearing for the orbiting scroll: Because the orbiting scroll is pushed to the fixed scroll by a back pressure, this loss is produced at the end plate surface. This loss is calculated by using the pressing force and the friction coefficient. The pressing force is calculated by using the simulated gas forces, and the friction coefficient is experimentally determined.

(4) Motor loss: The motor's efficiency is calculated from the experimental characteristics.

(5) Fluid resistance losses: Due to the orbiting scroll end plate and the balancing weight.

(6) Leakage loss: Leaked gas from the high pressure side into the compression chamber is re-compressed, resulting in compression losses. Leaked gas from the compression chamber to the suction side results in volumetric efficiency loss.

(7) Suction gas heating loss: Rising suction gas temperature results in volumetric efficiency loss, as well as power loss due to differences in refrigerant properties.

The losses (5) to (7) are focused on in this paper.

There are four components in this compressor model. They are the compressor body, the motor, the oil, and the hermetic shell. There are also six gas passages. They are the suction pipe, the suction chamber, the compression chamber, the upper shell chamber, the lower shell chamber and the discharge pipe. The following assumptions hold for heat conduction and transmission.

(1) Heat is conducted at three positions. These positions are between the motor stator and hermetic casing; between the motor rotor, crank shaft and compressor frame; and between the compressor frame and hermetic shell.

(2) Heat of refrigerant gas is exchanged between all components intensively in the above mentioned six passages.

The oil flows from the oil tank in the hermetic shell to a passage in the crank shaft, the bearing, the back pressure chamber, the compression chamber, the upper shell chamber and the lower shell chamber in that order, and returns to the oil tank. A small amount of oil is discharged during the refrigeration cycle, and after circulations, returns to the suction chamber. The heat transmission of the oil between the

components is assumed as follows.

(1) The oil temperature becomes the same as the frame's while it passes through the back pressure chamber.

(2) The gas and the oil completely exchange heat with each other when they are mixed in a passage.

The heat generated in the shell is compression loss, mechanical loss and motor loss. The mechanical loss consists of bearing loss, friction loss of the scroll end plate, and fluid resistance loss of the end plate and the balancing weight. The temperatures at any point are settled by the balance of heat exchange in the hermetic shell.

GAS COMPRESSION MODEL

The pressure in the compression chamber is calculated on the assumption that the gas is the perfect gas. The calculation model is shown in Figure 2. In order to calculate gas leakage with oil from the discharge chamber to the back pressure chamber through the bearing clearance, a leak port is assumed to be an integrated bearing clearance. The diameter of this port is determined to be an experimental parameter. The leakage and the heating of gas in the compression chamber are also considered. There is an alternative gas flow between the compression chamber and the back pressure chamber through the back pressure port.

According to volume change of the compression chamber and mass change of the gas by leakage in or out of the chamber, the pressure change is shown by equation (1).

$$\frac{dp}{p} + \kappa\left(\frac{dV_c}{V_c} - \frac{dm_g}{m_g}\right) = 0 \qquad (1)$$

On the assumption that the equalized leakage port is a contracting nozzle with friction, the mass flow rate is calculated by equation (2).

$$\frac{dm_g}{dt} = \xi\, a_2 P_0 \sqrt{\frac{2g\kappa}{\kappa-1}\left[\left(\frac{P_2}{P_0}\right)^{2/\kappa} - \left(\frac{P_2}{P_0}\right)^{(\kappa-1)/\kappa}\right]} \Big/ \sqrt{RT_0} \qquad (2)$$

The ξ is a coefficient of frictional flow in a nozzle and calculated by equation (3).

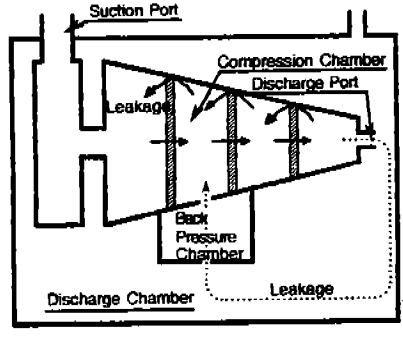

Fig. 2 Gas compression model

$$\xi = \sqrt{\left[\left(\frac{P_2}{P_0}\right)^{2/n} - \left(\frac{P_2}{P_0}\right)^{(n-1)/n}\right] \Big/ \left[\left(\frac{P_2}{P_0}\right)^{2/\kappa} - \left(\frac{P_2}{P_0}\right)^{(\kappa-1)/\kappa}\right]} \qquad (3)$$

Here, the n is the polytropic index calculated by equation (4).

$$n = \kappa(1+\zeta)/(1+\kappa\zeta) \qquad (4)$$

The ζ is the friction loss coefficient.

The friction loss of an end plate can be obtained from the differential force and friction coefficient of

the end plate. To estimate the differential force, accurate simulation of the back pressure is necessary.

A measured pressure of the back pressure chamber is compared with the calculated value. Figure 3 shows the change in back pressure ratio with driving frequency change. The reason the back pressure rises when the frequency becomes lower is because the leakage increases at lower frequency and the pressure in the intermediate compression chamber becomes higher. The calculated value agrees well with the measured value.

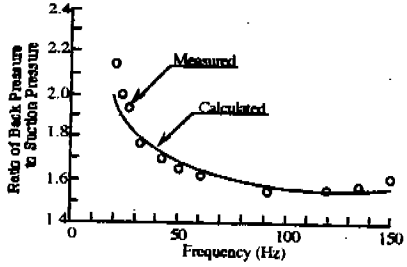

Fig. 3 Change in back pressure ratio

GAS LEAKAGE MODEL

The gas in the compression chamber leaks to a lower pressure chamber through the gap in the scroll wrap tip and the wrap flank. In this analysis, the leakage flow is assumed to conform to Moody's critical flow model. The mass flow rate is calculated by the equation of constant sectional area flow with friction (Fanno's flow model). For the wrap tip, the gap is constant from inlet to outlet. The gap of the wrap tip is described as a constant gap with an infinite width and a certain length in the model. For the wrap flank on the other hand, the gap changes along the passage. To simulate the gap of the flank, the passage is divided into about 100 cells, and it is assumed that the gap changes at each cell; however, the gap in one cell is constant.

The changing rate of Mach's number and pressure in the passage is shown by equations (5) and (6).

$$\frac{dM^2}{M^2} = \frac{\kappa M^2\left(1+\frac{\kappa-1}{2}M^2\right)}{1-M^2}\lambda\frac{dx}{D} \quad (5)$$

$$\frac{dP_0}{P_0} = -\frac{\kappa M^2}{2}\lambda\frac{dx}{D} \quad (6)$$

Using P_0 for the pressure and ρ_0 for the density when the flow velocity is 0, the actual pressure P and the actual density ρ are calculated in relation to the P_0 and the ρ_0, respectively, as shown by equations (7) and (8).

$$\frac{P}{P_0} = \left(1+\frac{\kappa-1}{2}M^2\right)^{-\frac{\kappa}{\kappa-1}} \quad (7)$$

$$\frac{\rho}{\rho_0} = \left(1+\frac{\kappa-1}{2}M^2\right)^{-\frac{1}{\kappa-1}} \quad (8)$$

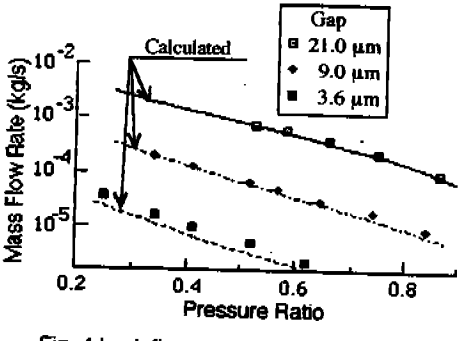

Fig. 4 Leak flow rate through constant gap

The mass flow rate is calculated by equation (9)

$$m = \rho VA = \rho MaA = \rho MA\sqrt{\kappa\frac{P}{\rho}} \quad (9)$$

These equations are solved by the Runge-Kutta-Gill method. The mass flow rate is obtained after the initial condition M has been satisfied, i.e., until the calculated pressure drop agrees with the inlet and outlet pressure difference.

The result of each calculation was verified by the constructive model test. Two types of models were used in this test. One type had a constant gap consisting of straight walls (wrap tip model), and the other had a changing gap consisting of curved walls (wrap flank model). The HCFC-22 was used as a fluid.

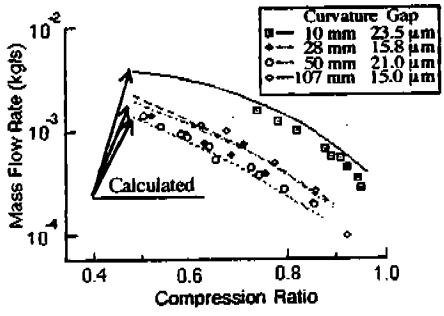

Fig. 5 Leak flow rate through curved wall gap

Leakage with pressure ratio change at the constant gap is shown in figure 4. The length of the passage is 4.5 mm and the width is 126 mm. The gap is changed from 0.0036 mm to 0.021 mm. The outlet pressure is 0.1 MPa and the pressure ratio of inlet to outlet is changed from 0.8 to 0.2. The calculated value agrees well with the measured value. The gap of the wrap tip is usually set from 0.005 mm to 0.015 mm for ordinarily produced compressors. As the tested range of gap covers the actual condition range, this calculation model is considered to be suitable for this analysis.

The result of a curved wall gap test is shown in Figure 5. The tested passage has a straight wall at one side and a curved wall at the other side. The width of the passage is 24.5 mm. The combination of wall curvature and gap is changed. The curvature is changed in 4 steps from 10 mm to 107 mm. The gap is also changed from 0.015 mm to 0.024 mm. The pressure condition is the same as the above case. The calculated value also agrees well with the measured value. The tested range of curvature and gap is cover the actual condition range for each, so this calculation model is considered to be suitable for this analysis.

HEAT EXCHANGE MODEL

A heat exchange model is shown in Figure 6. In this model, member 1 is an operating fluid (refrigerant with oil), member 2 is a passage for the fluid, and member 3 is one of the parts performing heat exchange with member 2.

In the suction pipe and the discharge pipe, the following Colburn's equation is used to obtain Nusselt's number Nu from Reinold's number Re and Prandtl's number Pr.

$$Nu = 0.023 Re^{4/5} Pr^{1/3} \quad (10)$$

On one hand, the other members are regarded as plates and the following Johnson-Rebesine's equation is used.

$$Nu = 0.0296 Re^{4/5} Pr^{2/3} \quad (11)$$

Member 1 receives heat quantity expressed by equation

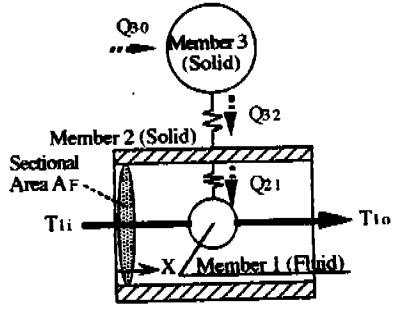

Fig. 6 Heat exchange model

(12).

$$Q_{21} = Gc_p(T_{1o} - T_{1i}) \tag{12}$$

On the other hand, the heat quantity transferred from member 2 to member 1 is calculated by equation (13).

$$Q_{21} = \alpha A_2(T_2 - \frac{T_{1i} + T_{1o}}{2}) \tag{13}$$

The heat quantity conducted from member 3 to member 2 is calculated by equation (14).

$$Q_{32} = \lambda_3 \frac{S}{L}(T_3 - T_2) \tag{14}$$

Q_{30} is motor loss, mechanical loss and compression loss when member 3 is the motor, the frictional component and the compression chamber respectively. The total heat balance is obtained as follows.

$$Q_{21}=Q_{32}=Q_{30} \tag{15}$$

The equations (12) to (15) are formed for all members, and they are simultaneously solved.

FLUID RESISTANCE MODEL FOR SCROLL AND BALANCING WEIGHT

In the compressor, the end plate of the orbiting scroll and the balancing weight have significant fluid resistances. These resistances come about since they stir the mixture fluid made from refrigerant gas and oil in the back pressure chamber.

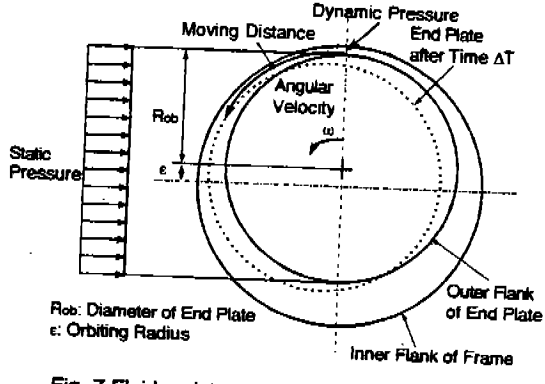

Fig. 7 Fluid resistance model of scroll end plate

To obtain the resistance loss of the end plate for the orbiting scroll, the model shown in Figure 7 is used. The periphery of the orbiting scroll's end plate is held between the fixed scroll and frame with a very slight gap. The orbiting motion produces a small radial gap between the flank of the orbiting scroll end plate and the inside flank of the frame shell at the biased point. This small gap revolves 1 time per 1 orbit of the scroll. The fluid around the end plate also circulates around 1 time by rotary pumping action of the end plate. It is considered that a dynamic pressure is generated in the small gap in proportion to the moving speed of the fluid. The dynamic pressure is considered to be converted to a static pressure in the other part. Then, the pressure difference between front flank and rear

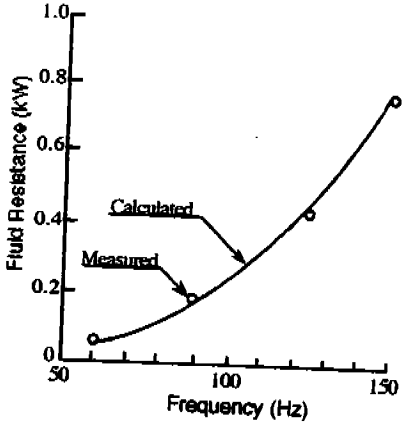

Fig. 8 Fluid resistance loss of end plate

flank of the end plate agrees with the above dynamic pressure. On the assumption that the pressure difference acts evenly on the front half flank, the loss caused by the above resistance force is calculated by equation (16).

$$L_{OB} = \omega \varepsilon D_{OB} H_{OB} \frac{\rho}{2} \{\omega (\frac{D_{OB}}{2} + \varepsilon)\}^2 \qquad (16)$$

Here, D_{OB} is the diameter of the end plate and H_{OB} is the height of the end plate flank.

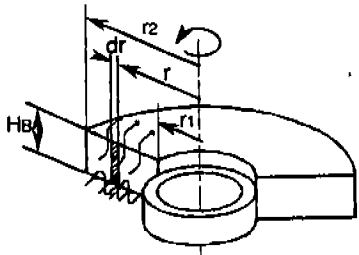

Fig. 9 Fluid resistance model of balancing weight

A measured resistance loss of the end plate is compared with a calculated value. The result is shown in Figure 8. The measured resistance loss is converted to a power from the measured pressure change around the periphery of the scroll end plate. The calculated loss agrees with the measured value very well and it is known that the loss shows a rapid rate of increase at a higher driving frequency.

The balancing weight in the back pressure chamber rotates in a mixture of refrigerant gas and oil. The balancing weight is shown in figure 9. The balancing weight is shaped like a half disk, and agitates the fluid. Therefore, the front surface receives a resistance. This resistance and the loss are obtained by the following equation.

$$L_{BW} = C_D \int_{r_1}^{r_2} \frac{\rho}{2} r^3 \omega^3 H_B dr = \frac{\rho}{8} C_D H_B \omega^3 (r_2^4 - r_1^4) \qquad (17)$$

Here, H_B is the height of the balancing weight, r_1 is the outer radius of the weight, and r_2 is the inner radius of the weight.

ANALYSIS OF COMPRESSOR BEHAVIOR CONSIDERING HEAT EXCHANGE AND LOSSES

Loss analysis with frequency change

A scroll compressor for air conditioning is analyzed by this method. The displacement volume of the compressor is 38.4 cm^3, and its built-in volume ratio is 2.3. The result is shown by the continuous line in Figure 10. The power loss consists of bearing loss, friction loss of the scroll end plate, fluid resistance loss of the end plate and the balance weight, leakage loss, and heating loss.

On comparing the calculated value and the measured value for the volumetric effi-

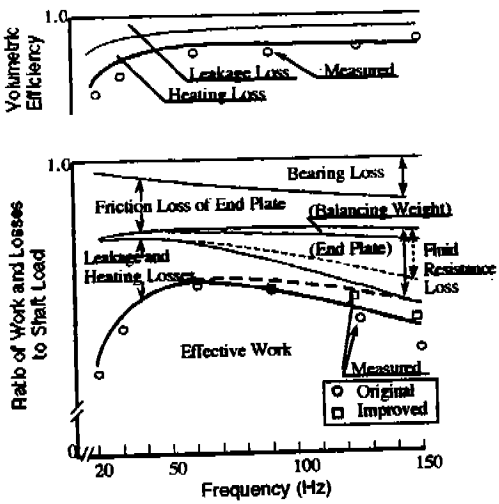

Fig. 10 Losses with frequency change

ciency, the tendency of both agree within 3% error. The calculated loss shows that the leakage loss and the heating loss are even below 50 Hz. However, the heating loss becomes double the leakage loss when the frequency rises over 100 Hz. This fact suggests that an effective way of improving volumetric efficiency is to reduce the heating of suction gas at any frequency.

On the other hand, with regard to power losses, the calculated value agrees well within 60 Hz to 120 Hz. The maximum error amounts to 3% under 60 Hz and over 120 Hz. The analyzed losses show that an effective way of reducing power losses is as follows.

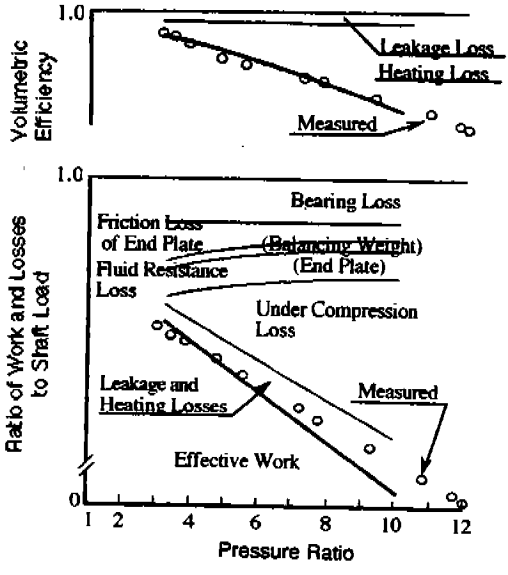

Fig. 11 Losses with pressure ratio change

At low frequency, an effective way is

(1) To reduce the leakage loss between compression chambers (about 36% of the total loss at 30 Hz now), or

(2) To reduce the friction loss of the end plate (about 38% of the total loss at 30 Hz now).

At high frequency, an effective way is

(3) To reduce the fluid resistance loss of the end plate (about 38% of the total loss at 150 Hz now), or

(4) To reduce both the bearing loss and the end plate friction loss (about 42% of the total loss at 150 Hz now).

To reduce the end plate friction loss, half of the end plate flank area, which receives fluid resistance, was cut out. The result is shown by the broken line in Figure 10. By analysis, it was understood that the end plate friction loss becomes about a half of its original the value. It was also understood that the adiabatic efficiency rises as much as the reduced value of the end plate friction loss.

Loss analysis with pressure ratio change

The frequency is set at a constant value of 125 Hz. The result is shown in Figure 11. The calculated and measured volumetric efficiency agree with each other. It is known that the main loss is the heating loss when the pressure ratio increases. The analyzed power loss also has a remarkable tendency. The per-

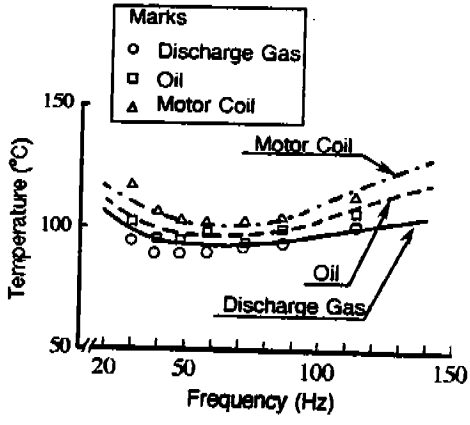

Fig. 12 Temperature with frequency change

centage of under compression loss greatly increases with increasing frequency. This loss can be omitted to some degree if a valve is attached on the discharge port. The calculated adiabatic efficiency agrees with the measured value within about 5% error.

Temperature analysis with frequency change

At the standard pressure and thermal condition, the driving frequency is changed. A comparison between calculated and measured temperature is shown in Figure 12. In the figure, the suction gas temperature, the discharge gas temperature, the oil temperature and the motor coil temperature are shown. The calculated discharge gas temperature, which is important for refrigeration cycle simulation, agrees with the measured value within 3 K. The result shows that the temperatures of high temperature parts are minimized between 40 Hz and 60 Hz. Figure 10 and Figure 12 clarify how losses affect temperature. The values of heat current between the members are also calculated by this analysis.

These overall analyses provide instruction regarding design and improvement of hermetic scroll compressors.

CONCLUSIONS

A practical method was developed to simulate the behaviors of hermetic scroll compressors accurately under wide conditions. The results are summarized as follows.

(1) To calculate the flow resistance loss at the scroll end plate periphery, a new method was developed to explain the pressure distribution. The calculated loss agrees well with the measured value.

(2) To calculate the leakage at the gap of a wrap tip and a wrap flank, Moody's critical flow model and Fanno's flow method were used. This method was validated by a leak test using an experimental model.

(3) The pressure in the back pressure chamber can be accurately calculated by the model considering the leak port is equivalent to an integrated bearing clearance.

(4) The temperatures at some points can be obtained by a simple heat circuit model considering the effect of oil. The calculated discharge gas temperature agrees with the measured value within 3K.

(5) By analysis, the overall power loss agrees with the experimental value within 3%.

REFERENCES

[1] K. Tojo, et al. "Computer Modeling of Scroll Compressor with Self-Adjusting Back-pressure Mechanism", Proc. of 1986 Compressor Engineering Conference at Purdue.

[2] N. Ishii, et al., "Mechanical Efficiency of Variable Speed Scroll Compressor", Proc. of 1990†Compressor Engineering Conference at Purdue.

[3] K. Suefuji, M. Shiibayashi, et al., "Deformation Analysis of Scroll Member in Hermetic Scroll Compressor for Air Conditioners", Proc. of 1988 Compressor engineering Conference at Purdue.

[4] M. Ikegawa, et al., "Scroll Compressor with Self-Adjusting Back Pressure Mechanism", ASHRAE Transactions, Vol. 90, Pt. 2, No. 2846, 1984.

[5] J. W. Bush and J. P. Elson, "Scroll Compressor Design Criteria for Residential Air conditioning and Heat Pump Applications", Proc. of 1988 Compressor Engineering Conference at Purdue.